

High temperature fiber pushout of pristine and transversely fatigued SiC/Ti-6-4

V. T. BECHEL*

Structural Materials Branch, AFRL/MLBC, 2941 P Street, Rm 136,
Wright Patterson AFB OH 45433-7750
E-mail: vernon.bechel@afrl.af.mil

N. R. SOTTOS

Theoretical and Applied Mechanics Dept., University of Illinois at Urbana, Champaign

An experiment was designed and constructed to perform fiber pushout tests at elevated temperatures in a controlled environment. Preliminary pushout tests on both a pristine and a transversely fatigued SiC/Ti-6-4 composite were conducted in atmospheric conditions to assess the capabilities of this apparatus and to study the interfacial behavior of SiC/Ti-6-4 at elevated temperature. At room temperature, the force-displacement behavior for the two types of samples was similar. The frictional portion of the load-displacement curve following total debond indicated that the interface could carry a greater load due to increasing friction and interlocking of the fiber and matrix surfaces. At 400 °C, significant changes in the load-displacement pushout curves were observed. At this elevated temperature, the interfacial friction produced by radial clamping was significantly reduced due to the relaxation of residual stresses, and significantly lower forces were required for pushout. The peak load for pushout of the fatigued samples at 400 °C was almost negligible, indicating that the fiber-matrix bond was broken by the fatigue loading. Due to varying compliance in the test fixture, it was not possible to identify progressive debonding. © 1999 Kluwer Academic Publishers

1. Introduction

Numerous research efforts have focused on the development of high performance, high temperature, metal matrix composites. Emphasis has been placed on strength, thermal stability, and oxidation resistance. Understanding the behavior of the fiber-matrix interface over a range of temperatures is essential for designing composites that will have a high service temperature. Several composites, such as silicon carbide or alumina fibers embedded in low density, high ductility titanium alloy, aluminum, or ceramic matrices are of current interest for high temperature applications. If the interface properties of these composites could be assessed as a function of temperature, it may be possible to determine why some fiber-matrix-coating combinations work well at high temperatures and why others do not.

Several studies of composite interface properties as a function of temperature have appeared in the literature. Chou *et al.* [1] performed fiber pullout tests on SiC fibers in two different glass matrices over a range of temperatures from room temperature to 500 °C. The interface strength was reported as the peak fiber pullout load divided by the fiber lateral surface area. Morscher *et al.* [2] performed fiber pushout tests on a SiC reinforced reaction-bonded silicon nitride

(RBSN) composite with a high temperature microhardness tester. A Vickers indenter was used to apply the pushout loads at temperatures up to 1350 °C. As in the work by Chou *et al.* [1], Morscher *et al.* [2] reported average shear stress as a function of temperature. Brun [3] conducted pushout tests on SiC fibers in mullite, cordierite, and titanium alloy matrices at temperatures up to 1100 °C in an argon atmosphere. The fibers were loaded with a 75 μm diameter flat faced punch which was less likely to damage the fibers than a sharp Vickers indenter, but the sample was supported only by the edges which were several fiber diameters from the fiber being pushed out. Elevated temperature fiber pushout tests were also carried out by Eldridge and Ebihara [4] and Eldridge [5]. Fiber pushout tests were performed in a vacuum chamber at temperatures that ranged from room temperature to 1100 °C on two different SiC/titanium alloy composites and on SiC/RBSN. Average interfacial shear stress was the criterion for interface failure.

Experiments recently reported by Bechel and Sottos [6] on model composites showed that a debond often grows through a large portion of the sample before the peak load is reached, making the average interfacial shear stress dependent on the sample thickness in the

* Author to whom all correspondence should be addressed.

fiber pushout test. In the work by Eldridge [5], interrupted pushout tests showed that fibers in the composites partially debonded at loads as low as 60% of the peak load also indicating that the average interfacial shear stress was dependent on sample thickness. Hence, using the average interfacial shear stress as a criterion for interface failure is ambiguous. Cordes and Daniel [7] observed the same type of sample thickness dependence in fiber pullout tests on a SiC/borosilicate glass composite.

Analyses more advanced than average interfacial shear stress have been developed to convert the force-displacement data from pushout experiments to interface properties. Liang and Hutchinson [8] and Kerans and Parthasarathy [9] developed a shear lag model to predict the interfacial critical energy release rate, G_{IIc} , from pushout data. Bechel and Sottos [10, 11] used an iterative finite element analysis to successfully predict the debond length during progressive debonding and to calculate G_{IIc} for model composites. The shear lag models could be used to determine the interfacial fracture energy at elevated temperatures if the measured displacement does not contain machine compliance and if the debond initiates at the top of the interface. The iterative finite element analysis could be used for a bottom debonding composite as well [11]. Unfortunately, all the previous high temperature fiber pushout work in the literature reports only the cross-head displacement since the primary goal was to measure the peak load.

In the absence of pushout data from previous high temperature pushout tests that would be appropriate for evaluating the interfacial toughness, an apparatus was developed to retrieve accurate load as well as displacement data from tests conducted in an environment that would simulate the service environment of metal matrix composites. The detailed design of the experimental apparatus is discussed as well as results from

preliminary pushout tests. Both pristine and laterally fatigued SiC/Ti-6-4 samples were tested at elevated temperature. Pushout curves containing identifiable progressive debonding were not obtainable, but modifications to the apparatus that may improve the measurement of the pushout data are outlined.

2. Experimental

2.1. Sample preparation

Pristine and fatigue loaded SiC/Ti-6-4 plates with 140 μm diameter fibers were fabricated at 3M Corporation. The lateral fatigue load on the fatigued composite consisted of 25,000 cycles at 180 MPa with an offset of $R = 0.1$ on samples that consisted of a 2 mm (thickness) \times 25 mm (width) \times 50 mm (length) gage section with 25 mm long end tabs. Inspection of the fatigued samples under a microscope revealed no signs of damage such as cracking or permanent deformation. The raw materials were sectioned with a diamond wafering saw into bars approximately 15 mm long, 2 mm wide, and 0.3 to 1.0 mm thick with the fibers aligned vertically (thickness direction). The top and bottom faces were ground parallel with 40 micron diamond particle sandpaper and polished to a 1 micron finish with diamond paste.

2.2. Apparatus

The high temperature fiber pushout device was modeled after the apparatus described in Eldridge and Ebihara [4] with significant differences in the optical system and sample and punch positioning equipment. A schematic of the tester is shown in Fig. 1. A vacuum chamber (A) was designed to house the experiment in a controlled atmosphere while allowing the test to be viewed in progress. A mechanical vacuum pump (Welch model

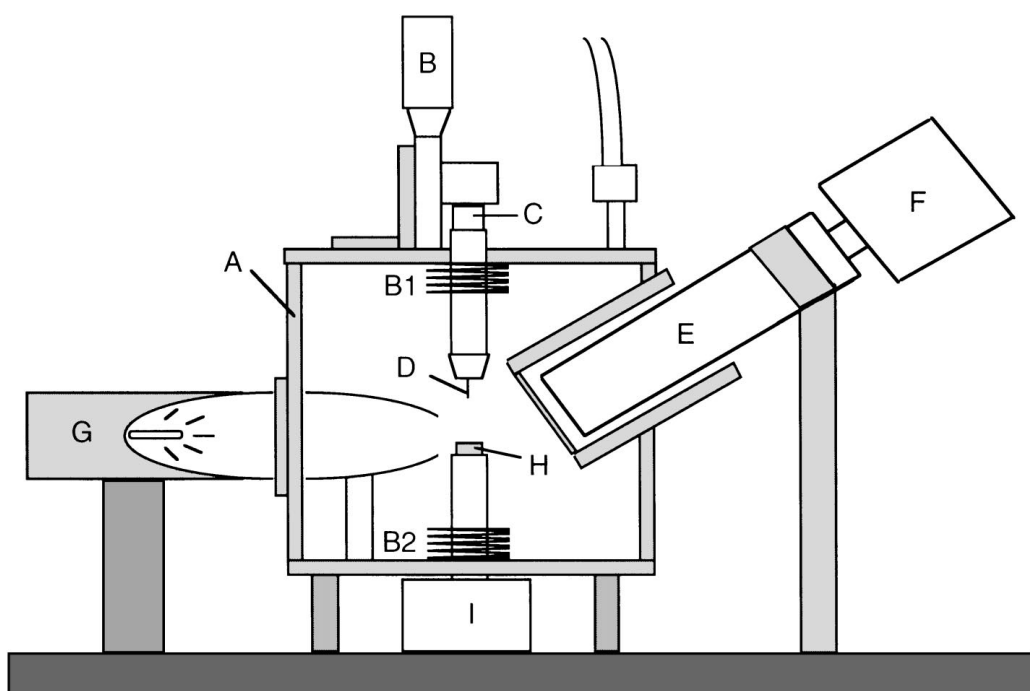


Figure 1 Schematic of the high temperature fiber pushout experiment.

1402) was available to reduce the pressure in the vacuum chamber to 10^{-3} Torr, after which the chamber could be flooded with high purity argon (10^{-6} impurity) to provide a virtually oxygen free atmosphere.

Bellows (B1 and B2) permitted vertical motion of the punch and motion of the sample table in three perpendicular directions. The punch (D) was attached to a motorized actuator (B) on the outside of the chamber while the sample support was attached to a three axis stage (I), which was also outside the chamber. The actuator consisted of a small DC motor turning a 10683 : 1 reducing gear box (Klinger, model BM4CC) that was mounted on a linear motion stage on the top flange of the chamber. When energized by the Newport PMC200 controller, the actuator drove the punch at a minimum velocity of 1.0 micron/second. Displacement of the probe was derived from the revolutions of the DC motor which were measured by an optical encoder on the motor's armature. The 105 μm diameter punch was machined from tungsten carbide (National Jet). The punch face that contacted the sample was flat, and the diameter of the punch shank increased slowly away from the flat face. A fiber could be moved at least 100 μm relative to the matrix before the sides of the punch touched the matrix.

Load was measured by sampling a Kistler piezoelectric charge transducer (C) at 5 samples/s. The load cell signal was conditioned by a Kistler dual mode amplifier and digitized by a Tektonix TDS 420 oscilloscope. The force versus cross-head displacement data were post-processed to account for load cell drift and machine compliance. For the range of loads applied during pushout testing (0 to 40 N) the approximate resolution of the load cell-amplifier-oscilloscope combination was ± 0.05 N.

The sample was heated by an infrared spot heater (Research, Incorporated, Model 4085). The heater (G) focused thermal energy generated by a lamp located at one focal point of an elliptical reflector into a one cubic centimeter volume engulfing the sample (H) at the other focal point of the reflector. Since the infrared heater required air cooling, the heater and the half of the reflector containing the lamp were located on the outside of the chamber next to a quartz window built into the wall of the chamber. The other half of the elliptical reflector was located inside the chamber on the opposite side of the quartz window. A quartz window was chosen because quartz is significantly more transparent to infrared light than glass. The maximum achievable sample temperature using this heater was not determined, but Eldridge and Ebihara [4] have reported pushout tests carried out at temperatures up to 1100 °C using similar equipment.

The sample temperature was measured by a thermocouple with its bead placed in contact with the steel and alumina sample support. A 200 μm hole was machined into the sample support to allow the bottom of the fiber to be stress free. The punch was attached to the upper bellows by an alumina ceramic rod to maintain thermal isolation of the sample. Similarly, an alumina rod supported the sample and rested on the lower bellows.

A long distance microscope (Infinity model K2) with a parfocal doubler and a 15X eyepiece (E) was

positioned inside a recessed glass window on the outside of the vacuum chamber opposite the infrared heater. The recessed window permitted the microscope objective to be within 5 cm of the sample and still be located outside the chamber. A black and white, high resolution CCD camera (580 horizontal lines) attached to the microscope obtained an image of the punch, the fiber(s) to be pushed out, and the surrounding area. A 10 cm extension tube placed between the camera (F) and the microscope further enlarged the image (without increasing the resolution). The image captured by the camera was displayed on a 12 inch monitor with 850 lines of resolution. The purpose of the video system was to aid in aligning the punch with the particular fiber that was over the support hole and to observe the pushout experiment in progress at temperatures below 150 °C. Observation of the test at temperatures above 150 °C required a filter because the light from the infrared heater saturated the CCD camera.

The capabilities of the long distance microscope and CCD camera system on the high temperature apparatus can be seen in Fig. 2. Fig. 2 is an image of the end of the tungsten carbide punch and the bottom face of a SiC/Ti-6-4 sample on which a fiber pushout test was previously conducted. A single fiber extends outward from the sample surface, and several untested fibers can be observed nearby.

3. SiC/Ti results

3.1. Pristine SiC/Ti-6-4

Pristine samples of SiC/Ti-6-4 were tested at room temperature and at 400 °C. An example of the cross-head displacement versus force at each temperature is shown in Fig. 3. At room temperature (23 °C), a drop in load (pt. A) was observed well before the peak load was reached. The fiber became totally debonded at the load drop, but the load increased another 8 N due to increasing friction in the interface before the decreasing embedded length caused the load to gradually decrease again. This phenomenon was also reported by Roman and Jero [12] for SiC/Ti-6-4 tested at room temperature and by Kantos *et al.* [13] for SiC/Ti-15-3. Kantos *et al.* [13] determined the cause of the increasing friction after total debond. Layers of carbon containing varying concentrations of SiC surround the SiC fiber. As the debond grows along the interface its path switches between these layers. Interlocking fiber and matrix surfaces are produced which crumble as the fiber is pushed out causing the friction between the fiber and matrix to increase for a period after total debond.

In the 400 °C curve shown in Fig. 3 the peak load was followed by a sharp load drop (pt. B) which signified total debond. The fiber was pushed further under a load which remained lower than the debond load. At 400 °C, the debond apparently chose a path that did not switch between layers since the pattern of increasing friction was not observed. Eldridge and Ebihara [4] observed similar trends for another metal matrix composite—SiC/Ti-15-3. At 23 and 300 °C interfacial friction increased after the peak load, and at 400 °C and

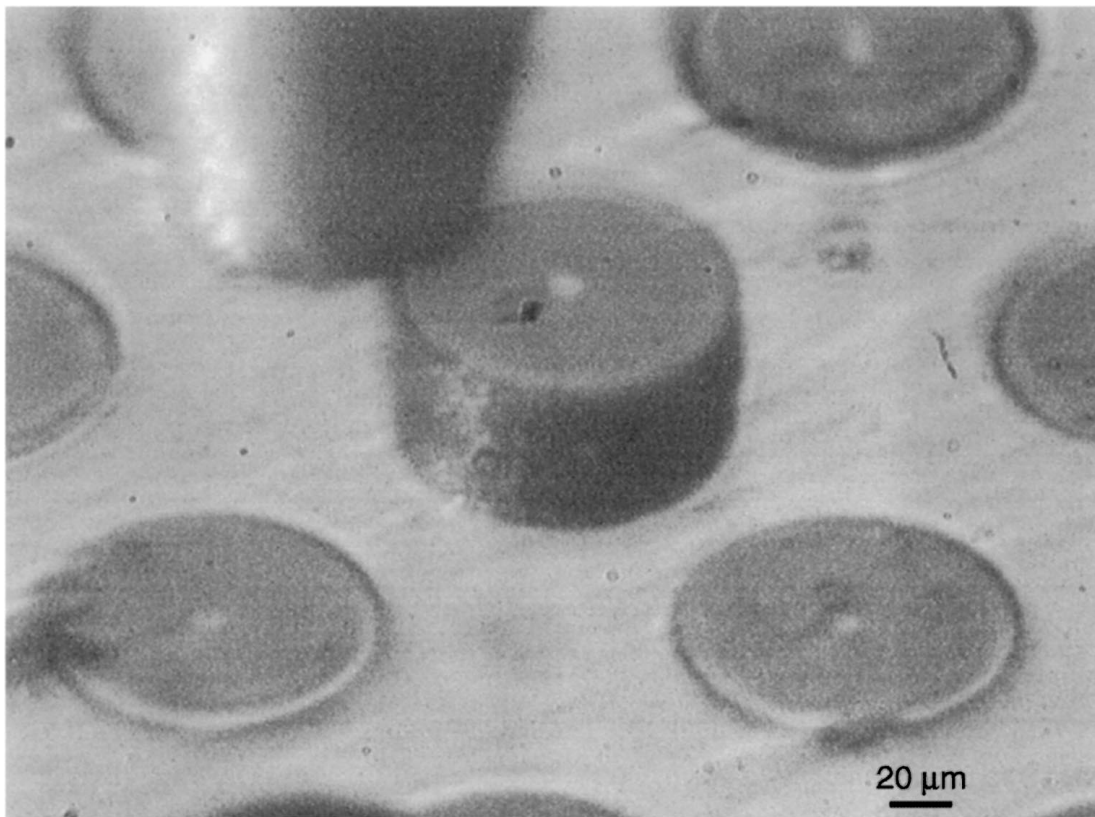


Figure 2 Punch and bottom surface of an SiC/Ti-6-4 composite with a single fiber pushed out.

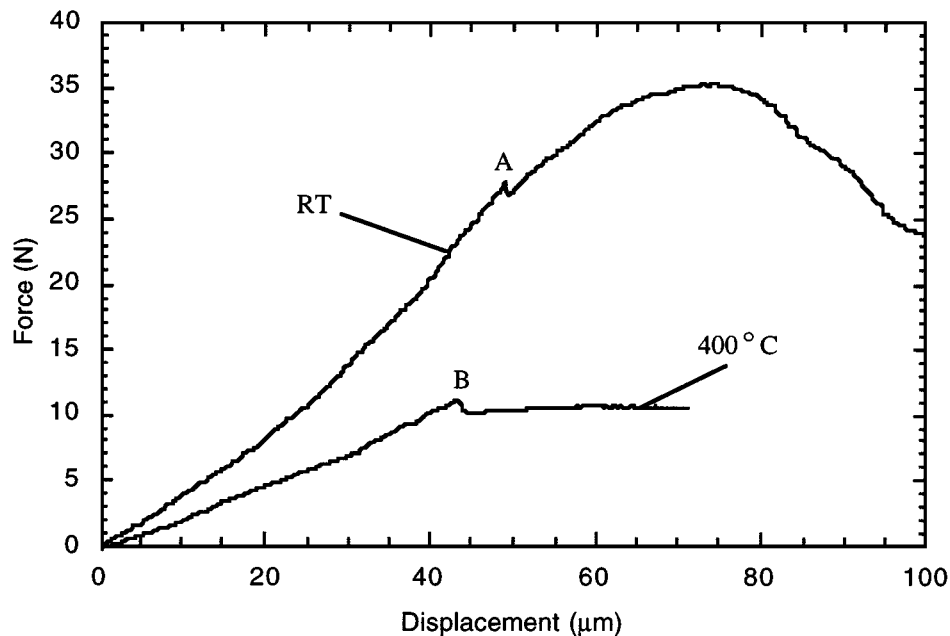


Figure 3 Force-displacement curves for pristine SiC/Ti-6-4 tested at room temperature (thickness = 0.39 mm) and at 400 °C (thickness = 0.30 mm).

above, the interface bond strength determined the peak load.

The samples appeared to stiffen when a load of approximately 8 N was reached (see Fig. 3). Machine compliance measurements were conducted by removing the punch and allowing the punch holder to engage the sample support while applying a load ranging from 0 to 40 N. The measurements of machine compliance revealed that the increase in slope was due to a decrease in fixture compliance at 8 N. After 8 N, the fixture compliance remained relatively constant. This observation highlights one of the difficulties in obtaining

accurate displacement measurements. If the events during the pushout test that are of interest (progressive debonding and frictional pushout) occur at loads low enough that all parts of the test fixture are not yet seated, it will be extremely difficult to separate the test fixture deflection from the displacement applied to the fiber surface.

3.2. Fatigued SiC/Ti-6-4

The results for the laterally fatigued SiC/Ti-6-4 composite are presented in Fig. 4. At room temperature, the

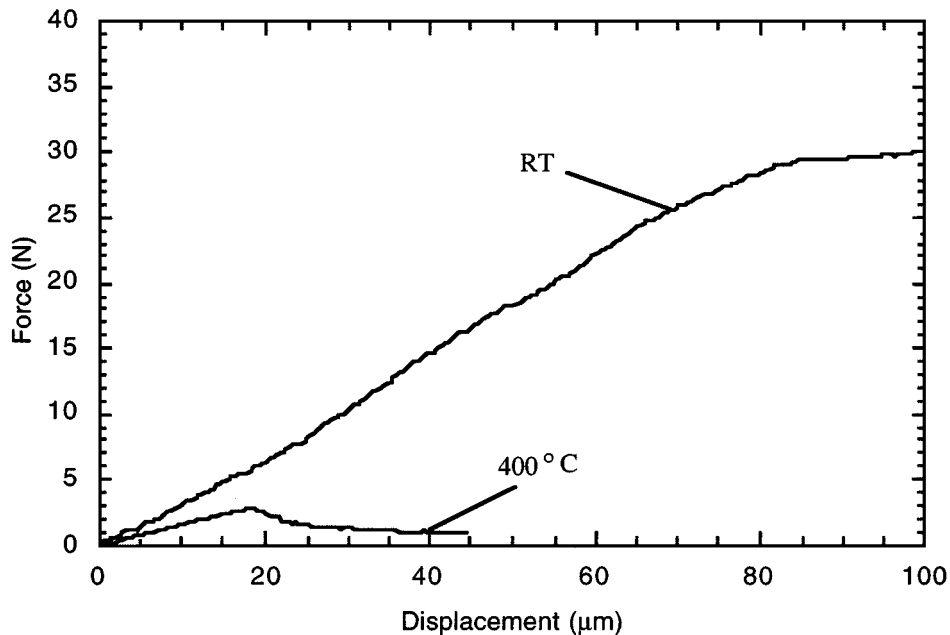


Figure 4 Pushout tests on fatigued SiC/Ti-6-4 at room temperature (thickness = 0.60 mm) and at 400 °C (thickness = 0.60 mm).

force-displacement curve was qualitatively the same as for the pristine SiC/Ti-6-4 except for the absence of a small load drop prior to the peak load. At 400 °C, the fiber in the 0.6 mm thick sample slid from the matrix under less than 3 N of applied load. By comparison, Fig. 3 shows that the peak load at 400 °C from a pristine sample of half this thickness was approximately 13 N. The lack of a sudden load drop in either the room temperature or high temperature tests on the fatigued samples indicates that the chemical bond between the fiber and matrix had been previously destroyed by the fatigue loading.

Several fibers were randomly chosen and pushout tested with similar results (no sudden load drop)—leading to the conclusion that all fibers in the fatigued sample had been completely debonded by the fatigue load. When a portion of the residual stresses was relieved at 400 °C, the interfacial friction produced by radial clamping became almost negligible. This conclusion is in agreement with results from tests done by Jansson *et al.* [14]. A static transverse load was applied to a SiC/Ti-6-4 composite while observing the exposed faces of the fibers under a microscope. At 200 MPa, a portion of the matrix surrounding some of the fibers separated from the fibers. The fiber-matrix interface closed upon unloading [14].

Warren *et al.* [15] applied a cyclic longitudinal load of 300 MPa ($R = 0.1$) to a SiC/Ti-15-3 composite. A matrix fatigue crack formed with the aid of a starter notch. Unlike the current results for *laterally* fatigued SiC/Ti-6-4, the pushout tests at room temperature conducted by Warren *et al.* [15] showed that only the fibers near the fatigue crack were debonded due to the *longitudinal* fatigue load.

At room temperature, the debonds in the laterally fatigued SiC/Ti-6-4 may not be detrimental to the performance of the composite unless, through loading and unloading of the composite, the interface wears and the load transfer due to friction between the fibers and

matrix reduces with time. On the other hand, at high temperature, preservation of the interfacial bond is critical since the chemical bond, and not friction, determines the limit on the magnitude of shear stress that can be transferred from the matrix to the fiber through the interface.

4. Progressive debonding in SiC/Ti

For room temperature pushout of SiC fibers from Ti-6-4, the issue of finding the interface fracture energy is, at best, ambiguous. The interface conditions on the surface of the debonded section of the fiber during progressive debonding are a combination of Coulomb friction and interaction of relatively large interlocking asperities. Also, asperities may break free as the pushout test progresses and build up nonuniformly along the interface. The shear lag and finite element analyses for calculating the interfacial toughness [8–10] assume Coulomb friction with a constant coefficient of friction in the debonded portion of the interface. Therefore, at room temperature, even if the force-displacement curve becomes nonlinear over some interval prior to total debond, the interfacial fracture energy could not be determined because the coefficient of friction may be varying significantly during progressive debonding. Also, Coulomb friction assumes that the length spacing of the asperities on the interface is uniform and much smaller than the distance that the fiber is moved. This assumption may also be violated. Kantos *et al.* [13] showed that the size of the interlocking asperities in the interface of SiC/Ti-15-3 can be on the order of the fiber radius.

As described earlier, the load drop at point A in the room temperature curve in Fig. 3 signifies total debond, and the force-displacement data after the sharp load drop are due to a debonded frictional interface. The frictional portion of the room temperature curve in Fig. 3 shows that, after total debond, the interface could carry

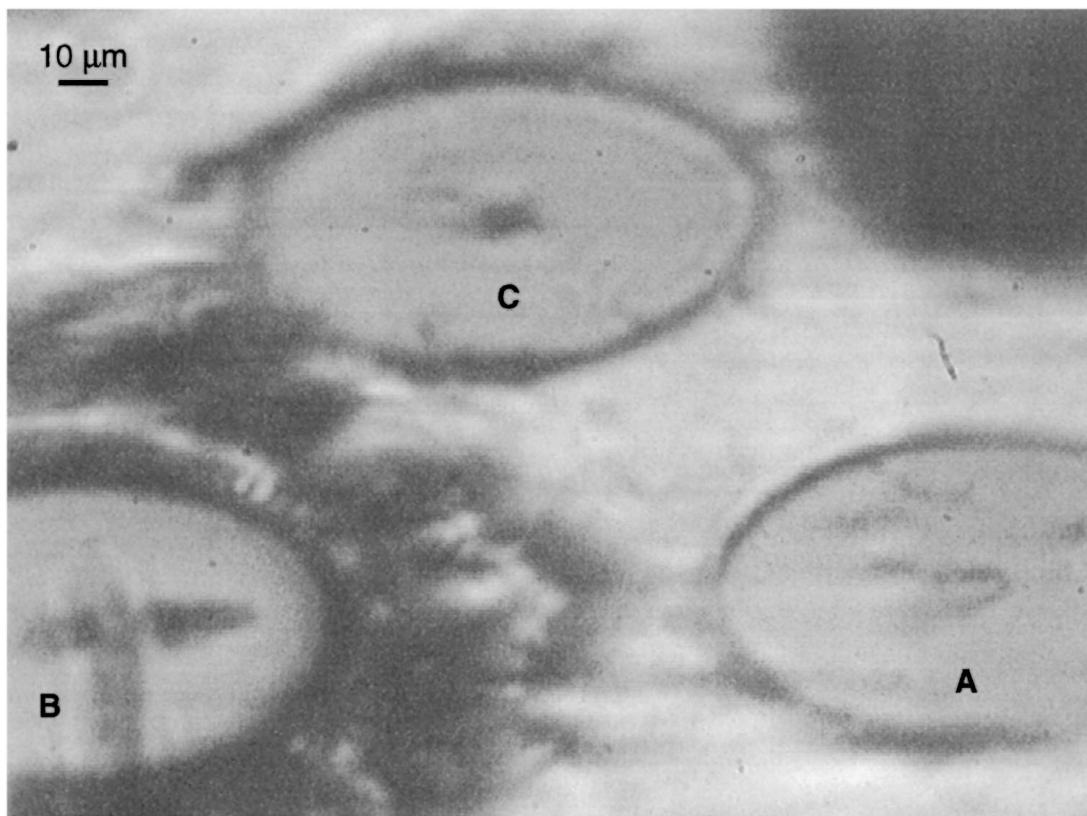


Figure 5 Three fibers in a pristine SiC/Ti-6-4 composite. Fiber A was not pushout tested. Fiber B was pushed out and back at room temperature. Fiber C was pushed out and back at 400 °C.

a greater load due to increasing friction and interlocking of the fiber and matrix surfaces. The chemical bond strength of the interface does not determine the maximum shear load that can be transferred from the matrix to the fiber. Consequently, if the interface bond strength is computed from the portion of the pushout data prior to the load at total debond (pt. A), the calculated strength may be excessively conservative since the interface can withstand much higher loads than are applied at total debond.

Calculating the interfacial toughness for SiC/Ti composites would be more straightforward at elevated temperatures. The peak load and total debond coincided for SiC/Ti-6-4 tested at 400 °C. The frictional portion of the pushout curve increased slightly over a displacement of 13 microns and leveled out as the fiber was pushed further. Fig. 5 shows an image of three of the SiC fibers. Fiber A was not pushout tested. Fiber B was pushed out at room temperature and pushed back at room temperature. Debris can be seen lying around the outer diameter of fiber B in a fan shape. This debris consisted of sections of the carbon/SiC layers originally coating the fiber that were sheared from the fiber during pushback and fell away from the fiber surface leaving a scatter of black pieces of carbon coating. The interlocking asperities on the fiber crumbled during pushout and were scraped from the fiber during pushback. In contrast, fiber C, which was pushed out at 400 °C and pushed back at 400 °C, had very little debris surrounding it. The lack of debris and the shape of the force-displacement curve indicate that at 400 °C the debond took a path between two of the SiC/carbon layers and did not jump between layers. The result is a

lack of interlocking surfaces—unlike the room temperature case. The interface conditions on the surface of the debonded portion of the fiber at 400 °C appeared to be closer to contact and sliding of two relatively smooth surfaces. If progressive debonding could be identified in the pushout curves from SiC/Ti-6-4 at 400 °C, then an interfacial toughness could be computed assuming no debonds were present prior to pushout testing.

The displacements in Fig. 3 have not been adjusted for machine compliance. Fig. 6 shows a portion of the high temperature test from Fig. 3 with the machine compliance of 2.47 μm/N removed. Assuming linear elastic deformation, the load-displacement curve from a pushout test should be linear above the load at which all parts of the test apparatus are aligned and seated (8 N for the current apparatus). A solid line has been fit through the curve in Fig. 6 to show that for loads above the 8 N the curve is mostly linear up to the peak load. The force-displacement curve deviates significantly from the line fit through the curve at 10.8 N and above 12 N. Measurements of machine compliance also revealed a variation of machine compliance near 10.8 and 12 N. Consequently the nonlinearity preceding the peak load cannot be attributed solely to progressive debonding. The nonlinearity was at least partially a result of a changing machine compliance. A stiffer and more uniformly linear test fixture response to loading is needed to determine if progressive debonding occurs in titanium matrix composites at high temperatures during fiber pushout tests.

Compliance tests showed that the gear box of the DC motor actuator was relatively compliant, and therefore a stepper motor and direct coupling between the stepper

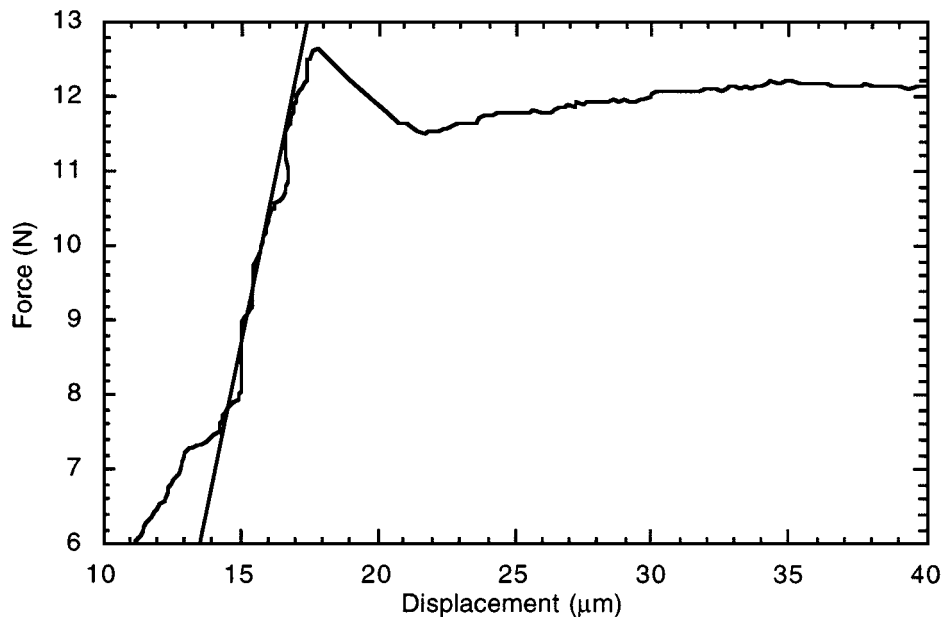


Figure 6 Pushout curve with machine compliance removed for pristine SiC/Ti-6-4 tested at 400 °C (thickness = 0.30 mm).

motor and the linear motion feedthrough (similar to the components used by Eldridge [5]) may be preferable. Several measurements of the effect on machine compliance of removing various parts of the structure of the high temperature apparatus also indicated that the three axis stage was responsible for a large portion of the test fixture compliance. Removal of the three axis stage also produced a much more uniform machine compliance beginning at a lower load. To remedy this problem the three axis stage should be replaced with a fixed sample support. An alternate method of aligning the fiber and punch would then be required. One possible solution would be to construct a sample transport outside the chamber that would extend into the chamber prior to the test and place the sample on the sample support such that the fiber is aligned with the punch.

5. Conclusions

Fiber pushout tests were conducted at room temperature and at 400 °C on a pristine and a transversely fatigued SiC/Ti-6-4 composite. For the pristine samples at room temperature a drop in load was observed well before the peak load was reached. The frictional portion of the load-displacement curve showed that, after total debond, the interface could carry a greater load due to increasing friction and interlocking of the fiber and matrix surfaces. At elevated temperature, the peak load was significantly lower than measured at room temperature and was followed by a sharp load drop. Increased friction was not observed after the load drop. At room temperature the path of the debond apparently switched between the carbon layers surrounding the SiC fiber creating interlocking fiber and matrix surfaces while at high temperature the debond did not alternate between layers.

The force-displacement curve for the laterally fatigued SiC/Ti-6-4 composite at room temperature was qualitatively the same as for the pristine sample except for the absence of a load drop prior to peak load.

At 400 °C, the value of the peak load in the fatigued samples was significantly lower than the peak load for the pristine samples at the same temperature. These results indicate that the transverse fatigue loading fully debonded the fibers. When the residual stresses were relaxed at elevated temperature, the interfacial friction produced by radial clamping was negligible and almost no resistance to pushout existed.

It was not possible to calculate interfacial toughness from the current pushout data. Modifications to the high temperature pushout apparatus may enable an experiment capable of identifying progressive debonding (if it exists) in SiC/Ti composites at high temperature. If progressive debonding data can be gathered, the interface strength as a function of temperature could be determined at elevated temperatures.

Acknowledgements

The authors would like to acknowledge the financial support of the ONR (under contract monitor R. Barsoum) and the AFOSR (Senior Knight Program). Also, we would like to acknowledge Dr. J. I. Eldridge from NASA Lewis for several helpful discussions about the design of the high temperature experiment.

References

1. H. M. CHOU, M. W. BARSOUM, and M. J. KOCZAK, *J. Mater. Sci.* **26** (1991) 1216.
2. G. MORSCHER, P. PIROUZ and A. H. HEUER, *J. Amer. Ceram. Soc.* **73** (1990) 713.
3. M. K. BRUN, *ibid.* **75** (1992) 1914.
4. J. I. ELDRIDGE and B. T. EBIHARA, *J. Mater. Res.* **9** (1994) 1035.
5. J. I. ELDRIDGE, *Mater. Res. Soc., Symp. Proc.* **365** (1995) 283.
6. V. T. BECHEL and N. R. SOTTOS, *J. Mech. Phys. of Solids* **46** (1998) 1675.
7. R. D. CORDES and I. M. DANIEL, *Comp. Eng.* **5** (1995) 633.
8. C. LIANG and J. W. HUTCHINSON, *Mech. of Mat.* **14** (1993) 207.

9. R. J. KERANS and T. A. PARTHASARATHY, *J. Amer. Ceram. Soc.* **74** (1991) 1585.
10. V. T. BECHEL and N. R. SOTTOS, *Comp. Sci. and Tech.* **58** (1998) 1727.
11. *Idem.*, *ibid.* **58** (1998) 1741.
12. I. ROMAN and P. D. JERO, *Mater. Res. Soc. Symp. Proc.* **273** (1992) 337.
13. P. KANTOS, J. I. ELDRIDGE, D. A. KOSS and L. J. GHOSN, *ibid.* **273** (1992) 135.
14. S. JANSSON, H. E. DEVE and A. G. EVANS, *Metal. Trans.* **22A** (1991) 2975.
15. P. D. WARREN, T. J. MACKIN and A. G. EVANS, *Acta Metal. et Mat.* **40** (1992) 1243.

*Received 11 February
and accepted 5 November 1998*